基于UPLC-Orbitrap-HRMS结合网络药理学分析心痛舒喷雾剂入血成分及治疗急性心肌梗死的作用机制

陆小龙[6], 李龙飞[7], 李平平[7], 梁万徽[6], 苏　梦[6], 左池靖[1,4,6], 张　静[1,3,6], 王　茜[6], 张云静[1,3,6,7], 彭　灿[1,2,3,4,5,6*]

(1. 安徽中医药大学, 新安医学与中医药现代化研究所, 安徽 合肥 230012;　2. 安徽中医药大学, 安徽省现代中药产业共性技术研究中心, 安徽 合肥 230012;　3. 安徽中医药大学, 安徽省乡村振兴协同技术服务中心, 安徽 合肥 230012;　4. 安徽中医药大学, 省部共建安徽道地中药材品质提升协同创新中心, 安徽 合肥 230012;　5. 安徽中医药大学, 药物制剂技术与应用安徽省重点实验室, 安徽 合肥 230012;　6. 安徽中医药大学药学院, 安徽 合肥 230012;　7. 华佗国药股份有限公司, 安徽 亳州 236000)

摘要: 为探明心痛舒喷雾剂治疗急性心肌梗死 (acute myocardial infarction, AMI) 的潜在活性成分及作用机制, 采用超高效液相色谱−四极杆−静电场轨道阱高分辨质谱法 (UPLC-Orbitrap-HRMS) 在正、负离子模式下检测, 分析鉴定心痛舒喷雾剂的入血原型成分与代谢产物, 结果共鉴定出41个入血原型成分, 其中有苯酞类16个、有机酚酸类15个、单萜类4个、苯乙酮类3个、香豆素类2个、糖类1个; 鉴定出46个代谢产物, 其中有22个苯酞类相关代谢产物、16个有机酚酸类相关代谢产物、苯乙酮类相关代谢产物7个、单萜类相关代谢产物1个。并结合网络药理学分析, 预测心痛舒喷雾剂入血成分治疗急性心肌梗死的作用靶点和信号通路, 结果表明, 有机酚酸类、苯酞类、单萜类为心痛舒喷雾剂治疗AMI的主要活性成分, 通过调控PI3K/Akt通路、AGE-RAGE通路、MAPK通路来治疗AMI。分子动力学模拟结果表明, 靶点蛋白与活性成分具有较好的结合能力。所有实验动物的使用取得了安徽中医药大学实验动物道德伦理委员会的批准 (批准号: AHUCM-rats-2021105)。

关键词: 心痛舒喷雾剂; UPLC-Orbitrap-HRMS; 入血成分; 急性心肌梗死; 网络药理学; 作用机制

中图分类号: R917　　**文献标识码**: A　　**文章编号**: 0513-4870(2025)10-3157-12

Exploring the blood-entry elements of Xintongshu spray and its mechanism of action in treating acute myocardial infarction using UPLC-Orbitrap-HRMS and network pharmacology

LU Xiao-long[6], LI Long-fei[7], LI Ping-ping[7], LIANG Wan-hui[6], SU Meng[6], ZUO Chi-jing[1,4,6], ZHANG Jing[1,3,6], WANG Qian[6], ZHANG Yun-jing[1,3,6,7], PENG Can[1,2,3,4,5,6*]

(*1. Center for Xin'an Medicine and Modernization of Traditional Chinese Medicine of IHM, Anhui University of Chinese Medicine, Hefei 230012, China;　2. Generic Technology Research Center for Anhui TCM Industry, Anhui University of Chinese Medicine, Hefei 230012, China;　3. Rural Revitalization Collaborative Technical Service Center of Anhui Province, Anhui University of Chinese Medicine, Hefei 230012, China;　4. MOE-Anhui Joint Collaborative Innovation Center for Quality Improvement of Anhui Genuine Chinese Medicinal Materials, Anhui University of Chinese Medicine, Hefei 230012, China;　5. Anhui Province Key Laboratory of Pharmaceutical Preparation Technology and Application, Anhui University of Chinese Medicine, Hefei 230012, China;　6. School of Pharmacy, Anhui University of Chinese Medicine, Hefei 230012, China;　7. Huatuo Chinese Medicine Co., Ltd., Bozhou 236000, China*)

Abstract: In order to investigate the potential active components and mechanism of action of Xintongshu Spray (XTS) in the treatment of acute myocardial infarction (AMI), ultra performance liquid chromatography-

收稿日期: 2025-02-14;　修回日期: 2025-07-21.

基金项目: 大健康研究院新安医学与中医药现代化研究所专项资金资助 (2023CXMMTCM006); 安徽省高校自然科学科研项目 (2023AH020035); 安徽省自然科学基金项目 (2408085J048); 安徽省科技创新攻坚计划项目 (202423I10050010); 国家中医药管理局高水平中医药重点学科中药资源学 (药用植物学) 建设项目 (zyyzdxk-2023095); 安徽高校协同创新项目 (GXXT-2022-075, GXXT-2022-084); 安徽省博士后科研项目 (2024C842).

*通讯作者 Tel: 86-551-68129155, E-mail: pengcanking@hotmail.com

DOI: 10.16438/j.0513-4870.2025-0142

quadrupole-electrostatic field orbital trap high-resolution mass spectrometry (UPLC-Orbitrap-HRMS) was used to analyze and identify the blood-entry prototype components and metabolites of XTS in both positive and negative ion modes. A total of 41 blood-entry prototype components and metabolites were identified, including 16 phthalides, 15 organic phenolic acids, 4 monoterpenes, 3 acetophenones, 2 coumarins, and 1 sugar; 46 metabolites were identified, including 22 phthalide-related metabolites, 16 organic phenolic acids, 7 acetophenone-related metabolites, and 1 monoterpene-related metabolite. Combined with network pharmacological analysis, the target of action and signaling pathway of XTS into blood components for the treatment of AMI were predicted. The results showed that organic phenolic acids, phthalides, monoterpenes are the main active components of XTS for AMI, through the regulation of PI3K/Akt pathway, AGE-RAGE pathway, MAPK pathway to treat AMI. The results of molecular dynamics simulation showed that that the target proteins have good binding ability with the active ingredients. The use of all experimental animals has been approved by the Ethics Committee of Laboratory Animal of Anhui University of Traditional Chinese Medicine (AHUCM-rats-2021105).

Key words: Xintongshu spray; UPLC-Orbitrap-HRMS; blood entry component; acute myocardial infarction; network pharmacology; mechanism of action

急性心肌梗死 (acute myocardial infarction, AMI) 是冠状动脉急性缺血、缺氧, 从而导致心肌细胞凋亡及损伤[1]。中医认为AMI属“真心痛”、“厥心痛”等范畴[2], 因痰浊、瘀血阻于心脉, 闭塞不通, 营气不行, 内陷腠理, 心失所养而发[3]。心痛舒喷雾剂是由川芎、牡丹皮和冰片三味中药制备而成的经舌下给药的溶液型喷雾剂 (Xintongshu spray, XTS, 批准文号: 国药准字Z20194075), 其经舌下毛细血管吸收后直接进入体循环, 起效快, 在心血管病急救方面具有独特优势。该制剂中川芎[4]是常用的活血化瘀药, 酚类和有机酸类、苯酞类化合物、生物碱类是川芎中的主要药效成分。其中有机酸类成分阿魏酸具有降低血小板聚集、改善急性心肌缺血、增强免疫等作用, 在临床上被广泛用于治疗心脑血管系统、血液系统等方面的疾病。牡丹皮具有清热凉血、活血化瘀的功效, 其化学成分主要包括苯乙酮类、萜类及其苷类、有机酸类以及其他类成分。现代药理研究表明, 牡丹皮中丹皮酚可通过抑制血小板聚集、抗调理素以及稳定红细胞膜等抑制血栓的形成[5]。冰片具有发散助气上行、醒神开窍的功效, 在治疗心脑血管疾病发挥着重要作用[6]。临床研究已证实XTS对各种类型及程度的AMI、冠心病所致的临床症状均有显著改善作用[7,8]。

中药血清药物化学理论认为吸收入血且达到一定血药浓度的成分被认为是发挥药效作用的活性成分。既往研究表明药物在正常和病理状态下的吸收代谢存在显著差异[9], 基于此, 本研究构建了大鼠AMI模型, 在课题组前期对XTS的质量控制[10]及体外化学成分研究的基础上, 进一步探究XTS在AMI大鼠体内化学成分变化, 探明其体内物质基础, 并结合网络药理学, 构建“入血原型成分−靶点−通路−疾病”网络, 系统分析XTS治疗AMI的潜在药效成分及作用机制, 为后续XTS的机制研究提供科学的理论依据和实验参考。

材料与方法

仪器 Exploris120 Orbitrap-HRMS仪和Vanquish UPLC仪 (美国Thermo Fisher公司); BT25S型十万分之一电子天平 (北京赛多利斯科学仪器有限公司); BL-420N生物信息采集分析系统 (成都泰盟仪器有限公司); Cascada超纯水仪 (美国PALL公司); 超低温冷冻储存箱 (中科美菱底纹科技有限公司); TDZ-WS型离心机 (长沙湘仪离心机仪器有限公司); YL-060S型超声波清洗机 (济南巴克超声波科技有限公司); 氮吹仪 (上海皓庄仪器有限公司); 石蜡包埋机 (孝感市亚光医用电子技术有限公司); 涡旋仪 (德国IKA公司)。

试剂 质谱级甲醇和乙腈 (美国Thermo Fisher公司); 质谱级甲酸 (国药集团化学试剂有限公司); 水为超纯水 (娃哈哈集团有限公司)。绿原酸、氧化芍药苷、阿魏酸、洋川芎内酯I对照品 (上海源叶生物科技有限公司, 批号分别为A22GB158496、N26GB169459、G13S11L124423、PZ7A11F122339, 纯度均 ≥ 98.0%); 咖啡酸、洋川芎内酯A、洋川芎内酯H、藁本内酯、芍药苷、丹皮酚、正丁基苯酞对照品 (成都普思生物科技有限公司, 批号分别为PS010522、PS011037、PS012143、PS012821、PS000825、PS000281、PS020613, 纯度均 ≥ 98.0%); XTS (华佗国药股份有限公司, 批号20220201); 乌来糖 (国药集团化学试剂有限公司, 批号C0029G); 伊红染色液、苏木素染色液 (Labcoms公司); 非吸收性外科缝线 (南通华利康医疗器械有限公司); 高纯氮气 (合肥聚辰化工有限公司); 手术器械 (泉州市医疗器械有限公司)。

动物 健康SPF级雄性Wistar大鼠30只, 体重

230 ± 20 g, 由济南朋悦实验动物繁育有限公司提供, 许可证号: SCXK (鲁) 20220006。动物实验取得了安徽中医药大学实验动物道德伦理委员会的许可, 伦理审批号为: AHUCM-rats-2021105。

AMI大鼠模型的构建 正常大鼠适应性饲养7天后, 第8天采用冠状动脉结扎法构建大鼠AMI模型[11], 用20%乌拉坦腹腔注射麻醉大鼠, 于左侧4、5肋间切口打开胸腔, 暴露心脏, 轻压胸廓挤出心脏, 用6-0号带线缝合针立即结扎冠状动脉左前降支根部 (肺动脉圆锥与左心耳处), 将心脏送回胸腔, 并轻挤出胸腔内气体和血液, 迅速关闭胸腔, 缝合皮肤, 打开胸腔时间不超过30 s, 待大鼠呼吸均匀后转移至鼠笼, 在术后36 h内需进行人工喂水喂食以提高存活率。

AMI大鼠模型心电图检测 在造模前和造模后4 h, 采用BL-420N生物信号采集与分析系统对每只大鼠进行心电图测定, 观察心电图ST段是否抬高, 以评价造模是否成功[12]。

心脏组织病理学检测 分别随机取造模前和造模后的心脏组织用4%多聚甲醛溶液固定并石蜡包埋, 取部分心肌按文献[13]所示方法进行苏木素-伊红染色 (hematoxylin and eosin, HE)。染色切片置于显微镜下观察并拍照, 应用CaseViewer软件分析图像。

分组与给药 将造模成功的AMI大鼠随机分为空白组和给药组, 每组各8只, 适应性喂养后开始灌胃给药, 给药组给予XTS, 空白组给予纯净水, 每天给药两次, 剂量均为10 mL·kg^{-1}, 连续给药3 d。

血清样品的采集与前处理 在末次给药前12 h, 大鼠禁食不禁水, 末次给药30 min后行腹主动脉取血, 血样静置1 h后, 4 ℃下转速3 500 r·min^{-1}离心10 min, 取上清液, −80 ℃保存。取空白组和给药组血清样品, 解冻后吸取同组血清合并做混合血清, 取混合血清0.5 mL, 加入3倍量乙腈沉淀蛋白, 涡旋10 min, 4 ℃下转速12 000 r·min^{-1}离心10 min, 取上清液, 氮气吹干, 残渣加入200 μL甲醇, 涡旋10 min, 4 ℃下转速12 000 r·min^{-1}离心10 min, 取上清液置于进样小瓶中待测。

液相色谱-质谱条件 Waters BEH C_{18}色谱柱 (100 mm × 3.0 mm, 1.8 μm), 流动相: 乙腈 (A)−0.1%甲酸水溶液 (B), 梯度洗脱程序: 0～3 min (5% A); 3～6 min (5%～13% A); 6～22 min (13%～30% A); 22～25 min (30%～36% A); 25～27 min (36%～60% A); 27～29 min (60%～5% A); 29～32 min (5% A), 流速0.4 mL·min^{-1}, 柱温35 ℃, 进样量5 μL。

电喷雾离子源 (ESI), 正、负离子检测模式, 质量扫描范围 *m/z* 100～1 500; 喷雾电压3 500/2 500V (−), 鞘气和辅助气均为氮气, 鞘气流速15 L·min^{-1}, 辅助气流速3 L·min^{-1}, 毛细管温度325 ℃, 气化温度350 ℃; full MS/dd-MS2扫描模式, 一级扫描分辨率60 000, 二级扫描分辨率30 000; 碰撞能梯度20、40、60 V。

数据处理与分析 采用Xcalibur qual browser 4.3软件, 基于实验室XTS体外化学成分鉴定结果及对照品图谱, 以空白组血清图谱作为背景, 鉴定给药组血清中的入血原型成分。将入血原型成分导入Compound Discoverer 3.3软件中, 再导入给药组和空白组图谱, 以空白组为背景, 选择“MetlD w Stats Expected w FlSh Scoring and Background Removal”处理流程, 检测给药组中的代谢产物。

网络药理学分析方法与分子对接验证 将XTS入血原型成分上传到Swiss Target Prediction数据库 (http://swisstargetprediction.ch/) 筛选得到入血原型成分作用靶点, 并通过UniProtKB数据库 (https://www.uniprot.org/uniprot/) 校正为标准基因名。以“acute myocardial infarction”为检索词, 检索Disgenet数据库 (http://disgenet.cn) 中与急性心肌梗死相关的靶点, 去除重复靶点后排序, 得到急性心肌梗死作用靶点。利用在线Venny2.1.0分析工具 (http://www.liuxiaoyuyuan.cn), 将XTS入血成分相关靶点与急性心肌梗死相关靶点导入, 得到交集靶点。将筛选得到的成分和疾病的共同靶点以基因通用名称的形式输入到STRING数据库 (https://string-db.org/), 隐藏游离靶点, 并选择中等置信度 > 0.4, 其余设置不变, 得到PPI网络及相关数据。将数据进一步导入Cytoscape 3.10软件, 计算度 (Degree) 值, Degree值越大, 说明节点在网络中越重要[14]。以Degree值 > 2倍中位数进行关键靶点筛选, 构建PPI网络图。将核心靶点上传至DAVID数据库 (https://david.ncifcrf.gov/), 进行KEGG通路富集分析, 得到相关通路, 汇总取前20位进行作图。对KEGG通路富集结果按照*P*由大到小排序, 进行数据可视化处理。对GO富集分析中生物过程 (biological process, BP)、细胞组分 (cell component, CC)、分子功能 (molecular function, MF) 相关通路进行数据可视化处理, 获得富集条形分析图。将筛选得到的核心活性成分作为配体, 核心靶点作为受体, 进行分子对接验证。分子对接的结合能 ≤ −5.00 kcal·mol^{-1}表明分子之间具有良好的结合活性[15]。

结果

1 大鼠AMI模型评价

1.1 心电图 将造模前与造模后的大鼠心电图进行对比, 发现造模后的大鼠心电图中ST段显著抬高, 表明造模成功。

1.2 HE染色 如图1所示，正常大鼠的心肌细胞排列整齐，细胞结构完整，无坏死现象，心肌纤维排列规则。AMI大鼠心脏的心肌细胞结构被破坏，核膜破损，细胞间质增大，炎性细胞浸润，出现坏死细胞，心肌纤维排列不规则，可观察到梗死灶，表明模型构建成功[16]。

2 XTS在AMI大鼠中原型成分鉴定

通过UPLC-Orbitrap-HRMS技术快速获取了含药组血清和空白组血清样品分别在正、负离子模式下的总离子流图。按照“数据处理与分析”项下方法进行分析鉴定，最终共鉴定出41个入血原型成分，其中有苯酞类16个，有机酚酸类15个，单萜类4个，苯乙酮类3个，香豆素类2个，糖类1个。入血原型成分的质谱信息见表1。

3 XTS在AMI大鼠中代谢产物鉴定

在含药组血清样品中共鉴定出46个代谢产物，其中有22个苯酞类相关代谢产物，16个有机酚酸类相关代谢产物，苯乙酮类相关代谢产物7个，单萜类相关代谢产物1个。各代谢产物的质谱鉴定信息见表2。以有机酚酸类相关的代谢产物为例，阐述有机酚酸类成分在AMI大鼠体内的代谢过程。

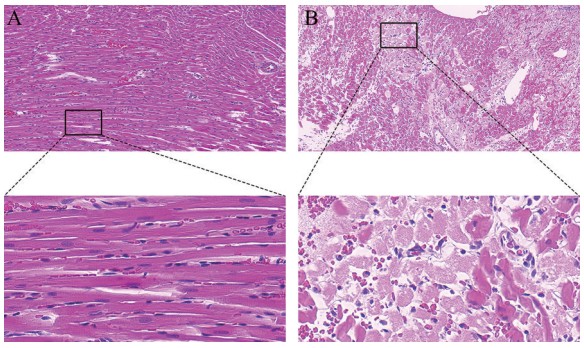


Figure 1 HE staining of myocardial histomorphology of rats before and after modeling (×400). A: The heart sections of normal rats; B: The heart sections of AMI model rats. HE: Hematoxylin and eosin; AMI: Acute myocardial infarction

Table 1 Prototype components in the serum of AMI model rats after administration of XTS. CX: Chuanxiong rhizome; MDP: Mudanpi; A: Phthalides; B: Organic phenolic acids; C: Monoterpenes; D: Acetophenones; E: Coumarins; F: Sugars; XTS: Xintongshu spray. *Confirmed by comparison with controls

No.	t_R /min	Identification	Formula	Ion mode	Observed (*m/z*)	Mass error ($\times10^{-6}$)	Fragment	Structure class	Origin
P1	1.08	Sucrose	$C_{12}H_{22}O_{11}$	$[M-H]^-$	341.108 8	3.2	179.056 3, 161.045 7, 119.035 1, 101.024 6, 89.024 5, 59.013 9	F	MDP
P2	1.13	Quinic acid	$C_7H_{12}O_6$	$[M-H]^-$	191.055 8	2.1	173.009 2, 129.019 4, 111.008 8, 85.029 4	B	CX
P3	1.64	Coumarin	$C_9H_6O_2$	$[M+H]^+$	147.044 0	−0.7	119.049 0, 91.054 1	E	CX
P4	6.09	Neochlorogenic acid	$C_{16}H_{18}O_9$	$[M-H]^-$	353.087 3	1.7	191.056 0, 179.034 9, 173.045 5, 135.045 2	B	CX
P5	7.02	4-Hydroxybenzaldehyde acid	$C_7H_6O_3$	$[M-H]^-$	137.024 0	4.4	93.034 6	B	MDP
P6	7.25	Paeoniflorin sulfite	$C_{23}H_{28}O_{13}S$	$[M-H]^-$	543.117 5	1.5	421.082 1, 375.075 8, 259.028 6, 213.023 0, 121.029 7	C	MDP
P7*	7.83	Oxypaeoniflorin	$C_{23}H_{28}O_{12}$	$[M-H]^-$	495.151 1	2.8	477.141 91, 465.142 27, 165.056 30, 137.024 96	C	MDP
P8*	7.91	Chlorogenic acid	$C_{16}H_{18}O_9$	$[M-H]^-$	353.088 0	3.7	191.056 0, 179.035 0, 173.045 4, 135.045 1	B	CX
P9	8.31	Cryptochlorogenic acid	$C_{16}H_{18}O_9$	$[M-H]^-$	353.088 0	3.7	191.055 9, 179.034 9, 173.045 5, 135.045 1	B	CX
P10*	8.65	Caffeic acid	$C_9H_8O_4$	$[M-H]^-$	179.034 3	2.2	135.045 1, 107.050 2	B	CX
P11	8.75	Vanillic acid	$C_8H_8O_4$	$[M-H]^-$	167.034 5	3.6	123.045 1, 79.055 4	B	CX
P12	9.31	Apiopaeonoside/ Phenolphthalein	$C_{20}H_{28}O_{12}$	$[M+Na]^+$	483.147 8	1.0	271.263 7, 167.071 5	D	MDP
P13	9.83	Apiopaeonoside/ Phenolphthalein	$C_{20}H_{28}O_{12}$	$[M+Na]^+$	483.147 0	−0.6	271.263 5, 167.071 6	D	MDP
P14*	10.83	Paeoniflorin	$C_{23}H_{28}O_{11}$	$[M+HCOO]^-$	525.161 5	2.3	449.145 0, 327.108 6, 165.055 7, 121.029 4	C	MDP
P15	11.06	4-Coumaric acid	$C_9H_8O_3$	$[M-H]^-$	163.039 9	4.9	145.890 3, 119.050 1, 93.034 5	B	CX
P16	12.27	6-Methoxycoumarin	$C_{10}H_8O_3$	$[M+H]^+$	177.054 4	−1.1	163.039 1, 149.059 7, 145.028 4, 117.033 6	E	CX
P17*	12.28	Ferulic acid	$C_{10}H_{10}O_4$	$[M-H]^-$	193.050 7	4.7	178.027 1, 149.060 7, 134.037 4	B	CX
P18	13.40	Isoferulic acid	$C_{10}H_{10}O_4$	$[M-H]^-$	193.050 6	4.1	178.027 0, 149.060 8, 134.037 4	B	CX

Continued

No.	t_R /min	Identification	Formula	Ion mode	Observed (*m/z*)	Mass error ($\times10^{-6}$)	Fragment	Structure class	Origin
P19	13.67	Senkyunolide S/R	$C_{12}H_{16}O_5$	$[M-H]^-$	239.092 4	4.2	227.892 7, 195.012 5, 177.092 2, 151.076 5	A	CX
P20	14.32	Senkyunolide J/N	$C_{12}H_{18}O_4$	$[M+Na]^+$	249.110 2	2.0	227.127 7, 209.117 1, 191.106 6, 153.054 5	A	CX
P21	14.73	Senkyunolide G/K	$C_{12}H_{16}O_3$	$[M+H]^+$	209.117 0	−1.0	191.106 7, 163.111 8, 153.054 6	A	CX
P22	15.46	Senkyunolide S/R	$C_{12}H_{16}O_5$	$[M-H]^-$	239.092 1	2.9	195.012 6, 177.092 1	A	CX
P23	15.54	Salicylic acid	$C_7H_6O_3$	$[M-H]^-$	137.023 2	−0.7	93.034 5	B	CX
P24	15.80	Senkyunolide F	$C_{12}H_{14}O_3$	$[M+H]^+$	207.101 4	−1.0	189.091 0, 161.096 0, 147.080 4, 119.085 6, 105.069 9	A	CX
P25	15.90	Senkyunolide G/K	$C_{12}H_{16}O_3$	$[M+H]^+$	209.117 6	1.9	191.106 8, 153.054 5	A	CX
P26	15.94	Azelaic acid	$C_9H_{16}O_4$	$[M-H]^-$	187.097 2	3.7	169.087 0, 125.097 2	B	CX
P27*	17.00	Senkyunolide I	$C_{12}H_{16}O_4$	$[M+Na]^+$	247.094 0	−1.6	225.113 2, 207.103 0, 189.092 5, 179.108 1, 161.097 2	A	CX
P28	17.81	Senkyunolide D	$C_{12}H_{14}O_4$	$[M+H]^+$	223.096 9	1.8	205.086 3, 177.091 4, 149.059 7	A	CX
P29*	18.08	Senkyunolide H	$C_{12}H_{16}O_4$	$[M+Na]^+$	247.094 4	0.0	225.112 3, 207.102 9, 189.092 7, 179.107 9, 151.112 8	A	CX
P30	18.30	Butylparaben	$C_{11}H_{14}O_3$	$[M-H]^-$	193.086 5	3.1	150.032 2, 136.016 7, 108.021 8	B	CX
P31	23.87	Benzoylpaeoniflorin	$C_{30}H_{32}O_{12}$	$[M-H]^-$	583.182 6	2.7	553.173 7, 431.136 7, 165.056 2, 121.029 8	C	MDP
P32*	24.47	Paeonol	$C_9H_{10}O_3$	$[M+H]^+$	167.070 3	0.0	149.060 41, 121.064 8, 43.0180 5	D	MDP
P33	24.84	Coniferyl ferulate	$C_{20}H_{20}O_6$	$[M-H]^-$	355.118 7	3.1	311.128 6, 281.081 8, 235.076 3, 173.060 5	B	CX
P34	26.86	Butylidenephthalide or isomer	$C_{12}H_{12}O_2$	$[M+H]^+$	189.091 4	2.1	161.096 2	A	CX
P35	27.09	*E*-Ligustilide	$C_{12}H_{14}O_2$	$[M+H]^+$	191.106 9	1.5	173.096 1, 163.112 1, 149.059 5, 145.101 3, 135.044 1	A	CX
P36	27.84	4-Hydroxy3-butylphthalide	$C_{12}H_{14}O_3$	$[M+H]^+$	207.101 9	1.7	189.090 9, 161.096 0, 147.080 3, 133.064 7, 105.069 8	A	CX
P37*	28.46	*Z*-Ligustilide	$C_{12}H_{14}O_2$	$[M+H]^+$	191.106 9	1.5	173.096 1, 163.112 1, 149.059 5, 145.101 3, 135.044 0	A	CX
P38	28.47	Senkyunolide B	$C_{12}H_{12}O_3$	$[M-H]^-$	203.070 8	2.5	174.032 4, 145.029 7, 132.022 0	A	CX
P39	28.84	13-Hydroxy-9,11-octadecadienoic acid	$C_{18}H_{32}O_3$	$[M-H]^-$	295.228 0	4.1	277.217 2, 195.138 8	B	CX
P40*	29.35	Senkyunolide A	$C_{12}H_{16}O_2$	$[M+H]^+$	193.122 6	1.6	175.111 7, 147.116 8, 137.059 6, 105.069 8	A	CX
P41*	30.29	3-Butylphthalide	$C_{12}H_{14}O_2$	$[M+H]^+$	191.106 5	−1.1	173.096 2, 163.111 9, 149.059 8, 135.044 1	A	CX

共鉴定出16个有机酚酸类相关的代谢产物, 其中包括个6咖啡酸代谢产物, 4个阿魏酸代谢产物, 3个没食子酸代谢产物, 3个香草酸代谢产物。绿原酸是XTS中重要的二聚体有机酚酸类成分, 有研究表明[17-19]绿原酸仅有30%在胃和小肠中以原型成分的入血, 约有70%的绿原酸被传输到大肠或结肠, 肠道中的绿原酸在肠道菌群的作用下被水解为咖啡酸和奎宁酸并被吸收, 经进一步代谢排出体外, 因此推测咖啡酸和奎宁酸既是入血原型成分, 同时也是绿原酸的代谢产物。*m/z* 179.0347 $[M-H]^-$是咖啡酸的母离子, 其碎片离子为*m/z* 135.0451 $[M-H-CO_2]^-$; 代谢产物M7的母离子为*m/z* 355.066 7 $[M-H]^-$, 分子质量比咖啡酸多176 Da (GluA), 同时可见*m/z* 179.034 9 $[M-H-C_6H_8O_6]^-$和*m/z* 135.045 1 $[M-H-C_6H_8O_6-CO_2]^-$的咖啡酸特征碎片离子, 推测为咖啡酸葡萄糖醛酸化产物; 代谢产物M12母离子为*m/z* 369.081 8 $[M-H]^-$, 分子质量比咖啡酸多190 Da (GluA+CH_2), 且发现脱去一分子葡萄糖醛酸的*m/z* 193.0504 $[M-H-C_6H_8O_6]^-$碎片离子、再脱去一分子甲基的*m/z* 178.0270 $[M-H-C_6H_8O_6-CH_3]^-$及再脱去羧基的*m/z* 134.037 3 $[M-H-C_6H_8O_6-CH_3-CO_2]^-$碎片离子, 推测为咖啡酸的甲基化和葡萄糖醛酸化代谢产物, 由于未见*m/z* 149 $[M-H-C_6H_8O_6-CO_2]^-$碎片离子, 推测甲基结合在咖啡酸的羧基上。同理参考相关文献[20-22]结合质谱裂解规律可推测M4为二氢咖啡酸; M8为咖啡酸的硫酸化代谢产物; M10为咖啡酸甲基化和硫酸化代谢产物。代谢产物M9的母离子为*m/z* 178.050 9 $[M-H]^-$, 碎片离子为*m/z* 134.061 1 $[M-H-CO_2]^-$, 根据文献[23,24]推测该代谢产物为马尿酸, 其为咖啡酸和奎宁酸在体内代谢成苯甲酸后再与甘氨酸(Cly)结合的产物。

有报道[25]称, 咖啡酸可以在体内发生甲基化代谢反应从而生成阿魏酸和异阿魏酸, 因此阿魏酸和异阿魏酸可能既是入血原型成分, 同时也是咖啡酸的代谢产物。阿魏酸的母离子为*m/z* 193.050 5 $[M-H]^-$, 特征的碎片离子有 *m/z* 178.027 0 $[M-H-CH_3]^-$、*m/z* 149.060 7 $[M-H-CO_2]^-$和 *m/z* 134.037 3 $[M-H-CO_2-CH_3]^-$。代谢产物M6母离子为*m/z* 369.082 3 $[M-H]^-$, 分子质量比阿魏酸多176 Da (GluA), 同时可见 *m/z* 193、178、149和134等阿魏酸特征碎片离子, 推测为阿魏酸葡萄糖醛酸化产物; 代谢物M13的母离子为*m/z* 273.007 3 $[M-H]^-$, 分子质量比阿魏酸多80 Da (SO_3), 同时可见 *m/z* 193、178、149和134等阿魏酸特征碎片离子, 推测为阿魏酸硫酸酯化产物。同理参考相关文献[26,27]结合质谱裂解规律可推测M15为阿魏酸甘氨酸 (Cly) 结合产物; M31为阿魏酸酸二甲基化代谢产物。上述各代谢产物的提取离子流图和在大鼠体内可能的代谢途径见图2、3。

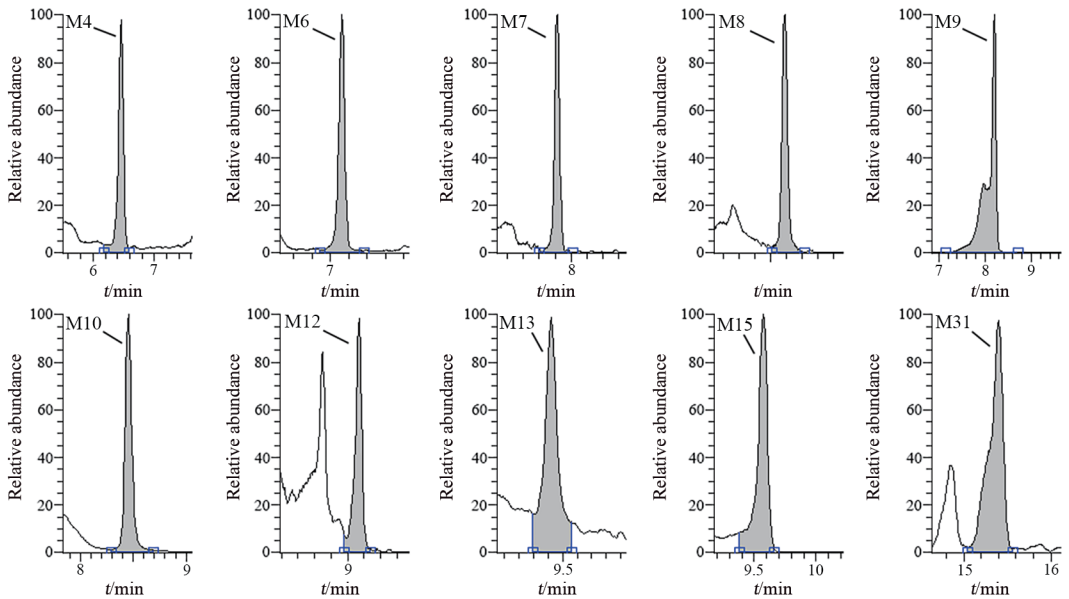


Figure 2 Extracted ion chromatograms of organic acid-related metabolites. Details of M4, M6, M7, M8, M9, M10, M12, M13, M15, M31 are shown in Table 2

Table 2 Metabolites in the serum of AMI model rats after administration of XTS

No.	t_R /min	Metabolite description	Formula	Measured ion (*m/z*)	Mass error ($\times10^{-6}$)	Fragment ion (*m/z*)
M1	3.34	Gallic acid+Sulfate conjugation	$C_7H_6O_8S$	248.971 4 $[M-H]^-$	4.8	169.013 9, 125.024 3
M2	5.44	Vanillic acid loss of CO_2+Sulfate conjugation	$C_6H_6O_5S$	188.986 1 $[M-H]^-$	4.8	109.029 4, 79.957 3
M3	5.63	Vanillic acid+Sulfate conjugation	$C_8H_8O_7S$	246.991 5 $[M-H]^-$	3.2	167.034 7, 152.011 5, 123.045 2, 108.021 5
M4	6.46	Caffeic acid+Di-hydrogenation	$C_9H_{10}O_4$	181.050 6 $[M-H]^-$	0.0	163.040 0, 135.045 2, 119.050 3
M5	6.67	Gallic acid+Methylation	$C_8H_8O_5$	183.029 5 $[M-H]^-$	3.8	168.006 3, 124.016 5
M6	7.12	Ferulic acid+Glucuronide conjugation	$C_{16}H_{18}O_{10}$	369.082 3 $[M-H]^-$	1.9	193.050 5, 178.027 0, 149.060 7, 134.037 3
M7	7.82	Caffeic acid+Glucuronide conjugation	$C_{15}H_{16}O_{10}$	355.066 7 $[M-H]^-$	−2.0	179.034 9, 135.045 2
M8	8.16	Caffeic acid+Sulfate conjugation	$C_9H_8O_7S$	258.991 6 $[M-H]^-$	−0.8	179.034 9, 135.045 2
M9	8.21	Benzoylglycine	$C_9H_9NO_3$	178.050 7 $[M-H]^-$	4.5	134.061 1
M10	8.47	Caffeic acid+Methylation+Sulfate conjugation	$C_{10}H_{10}O_7S$	273.007 4 $[M-H]^-$	0.0	193.050 6, 178.027 2, 134.037 4
M11	8.74	Paeonol+Demethylation+Glucuronide conjugation	$C_{14}H_{16}O_9$	327.072 4 $[M-H]^-$	4.0	175.024 8, 151.040 1, 113.024 5, 85.029 6
M12	9.14	Caffeic acid+Methylation+Glucuronide conjugation	$C_{16}H_{18}O_{10}$	369.081 8 $[M-H]^-$	0.5	193.050 6 178.027 1, 134.037 4
M13	9.44	Ferulic acid+Sulfate conjugation	$C_{10}H_{10}O_7S$	273.007 4 $[M-H]^-$	0.0	193.050 6, 178.027 0, 149.060 7, 134.037 4

Continued

No.	t_R /min	Metabolite description	Formula	Measured ion (*m*/*z*)	Mass error ($\times10^{-6}$)	Fragment ion (*m*/*z*)
M14	9.27	Gallic acid+Di-methylation+Glucuronide conjugation	$C_{15}H_{18}O_{11}$	373.077 1 $[M-H]^-$	2.4	197.045 4, 169.014 1, 125.024 3, 124.016 5
M15	9.60	Ferulic acid+Glycine conjugation	$C_{12}H_{13}NO_5$	250.071 9 $[M-H]^-$	3.6	206.082 0, 191.058 6, 177.055 4, 149.060 7, 134.037 4
M16	10.11	Paeonol+Hydroxylation+Glucuronide conjugation	$C_{15}H_{18}O_{10}$	357.082 2 $[M-H]^-$	1.7	181.050 6, 166.027 1, 138.032 1, 123.008 7, 113.024 4
M17	10.32	Paeonol+Demethylation+Sulfate conjugation	$C_8H_8O_6S$	230.996 8 $[M-H]^-$	4.3	151.040 1, 135.008 8, 109.029 5, 91.019 0
M18	10.33	Paeonol+Glucuronide conjugation	$C_{15}H_{18}O_9$	341.087 4 $[M-H]^-$	2.1	175.024 8, 165.055 6, 150.032 2, 113.024 4
M19	10.37	Paeonol+Hydroxylation+Sulfate conjugation	$C_9H_{10}O_7S$	261.007 3 $[M-H]^-$	3.8	181.050 6, 166.027 1, 138.032 1, 123.008 7
M20	10.57	Senkyunolide F+Sulfate conjugation	$C_{12}H_{16}O_7S$	303.054 3 $[M-H]^-$	3.3	223.097 4, 205.087 0, 177.092 0
M21	10.80	Paeoniflorin+Dehydroxylation+Demethylation	$C_{22}H_{26}O_{10}$	449.146 4 $[M-H]^-$	4.9	327.108 3, 165.055 7, 121.029 5
M22	10.95	Senkyunolide F+Sulfate conjugation	$C_{12}H_{16}O_7S$	303.054 1 $[M-H]^-$	2.6	223.097 2, 205.087 1, 177.091 9
M23	11.32	Paeonol+Sulfate conjugation	$C_9H_{10}O_6S$	245.012 3 $[M-H]^-$	3.7	165.055 6, 150.032 1, 122.037 2
M24	12.65	Senkyunolide D+Desaturation	$C_{12}H_{12}O_4$	219.065 9 $[M-H]^-$	3.2	175.076 2, 157.065 7, 133.065 9
M25	12.91	Senkyunolide A+Hydroxylation+Hydrolysis	$C_{12}H_{18}O_4$	227.127 2 $[M+H]^+$	−2.6	209.117 2, 191.106 7, 181.122 2, 163.111 8, 153.054 7
M26	13.18	Senkyunolide I/H+Hydroxylation+Glutathione conjugation	$C_{22}H_{33}N_3O_{10}S$	532.196 3 $[M+H]^+$	0.9	457.162 9, 403.154 4, 385.142 5, 367.133 0, 207.101 8
M27	13.34	*Z*/*E*-Ligustilide+Hydroxylation+Glucuronide conjugation	$C_{18}H_{22}O_9$	381.118 6 $[M-H]^-$	1.8	205.086 5, 187.076 2
M28	14.31	Senkyunolide J/N+Cysteine conjugation	$C_{15}H_{23}NO_5S$	330.137 0 $[M+H]^+$	0.0	284.131 5, 209.117 2, 191.106 6
M29	14.34	Paeonol+Demethylation	$C_8H_8O_3$	151.039 7 $[M-H]^-$	4.6	135.008 8, 109.029 5, 91.018 9, 65.039 7
M30	15.09	Senkyunolide J/N+Glutathione conjugation	$C_{22}H_{33}N_3O_9S$	516.200 7 $[M+H]^+$	−0.6	441.168 5, 387.158 4, 284.131 5, 191.106 7
M31	15.38	Ferulic acid+Di-methylation	$C_{12}H_{14}O_4$	221.081 7 $[M-H]^-$	4.1	177.091 8, 149.097 2
M32	15.53	Vanillic acid loss of CH_2O	$C_7H_6O_3$	137.023 9 $[M-H]^-$	−4.4	93.034 5
M33	16.01	Senkyunolide I/H+Cysteine conjugation	$C_{15}H_{21}NO_5S$	328.121 5 $[M+H]^+$	0.6	282.115 9, 207.101 5, 189.090 9
M34	16.79	*Z*/*E*-Ligustilide+Dehydrogenation+Glutathione conjugation	$C_{22}H_{29}N_3O_8S$	496.175 1 $[M+H]^+$	0.6	421.143 2, 367.132 1, 189.091 0
M35	16.87	Senkyunolide I/H+Glutathione conjugation	$C_{22}H_{31}N_3O_9S$	514.186 2 $[M+H]^+$	1.7	439.153 2, 385.142 6, 282.116 0, 207.101 5, 189.090 9
M36	16.88	Senkyunolide I/H+Cysteine conjugation+Glycine conjugation	$C_{17}H_{24}N_2O_6S$	385.143 0 $[M+H]^+$	0.5	282.115 9, 207.101 5, 179.048 3, 162.022 0
M37	17.33	*Z*/*E*-Ligustilide+Hydroxylation+Sulfate conjugation	$C_{12}H_{14}O_6S$	285.043 7 $[M-H]^-$	3.5	205.086 8, 177.029 0, 161.096 9
M38	17.54	*Z*/*E*-Ligustilide+Hydroxylation+Glucuronide conjugation	$C_{18}H_{22}O_9$	381.119 0 $[M-H]^-$	2.6	205.086 7, 161.096 9
M39	17.96	Senkyunolide A+Internal hydrolysis	$C_{12}H_{18}O_3$	211.132 9 $[M+H]^+$	0.0	193.122 3, 175.111 7, 165.127 5, 147.116 9
M40	18.45	Senkyunolide I/H+Methylation	$C_{13}H_{18}O_4$	239.127 4 $[M+H]^+$	−1.7	221.116 6, 207.101 5, 189.091 2, 179.106 4, 165.091 0, 137.096 1
M41	21.04	Senkyunolide I/H+Dehydroxylation+Di-hydrogenation	$C_{12}H_{20}O_3$	213.148 0 $[M+H]^+$	−2.4	195.138 7, 177.127 7, 149.132 5
M42	21.43	Senkyunolide I/H+Desaturation	$C_{12}H_{14}O_4$	223.096 5 $[M+H]^+$	0.0	205.086 1, 177.091 2, 167.033 9, 149.023 3
M43	22.95	Senkyunolide I/H+Acetycysteine conjugation	$C_{17}H_{23}NO_6S$	370.131 3 $[M+H]^+$	−1.6	352.122 2, 328.121 5, 282.116 3, 207.101 5, 189.090 9
M44	23.47	4-Hydroxy-3-butylphthalide+Methylation+Hydroxylation+Glucuronide conjugation	$C_{19}H_{24}O_{10}$	411.129 7 $[M-H]^-$	2.7	235.097 5, 203.071 3, 175.024 8
M45	23.77	4-Hydroxy-3-butylphthalide+Methylation+Hydroxylation+Glucuronide conjugation	$C_{19}H_{24}O_{10}$	411.129 8 $[M-H]^-$	2.7	235.097 5, 203.071 2, 175.024 9
M46	26.79	*Z*/*E*-Ligustilide+Hydroxylation	$C_{12}H_{14}O_3$	205.086 9 $[M-H]^-$	4.9	161.097 1

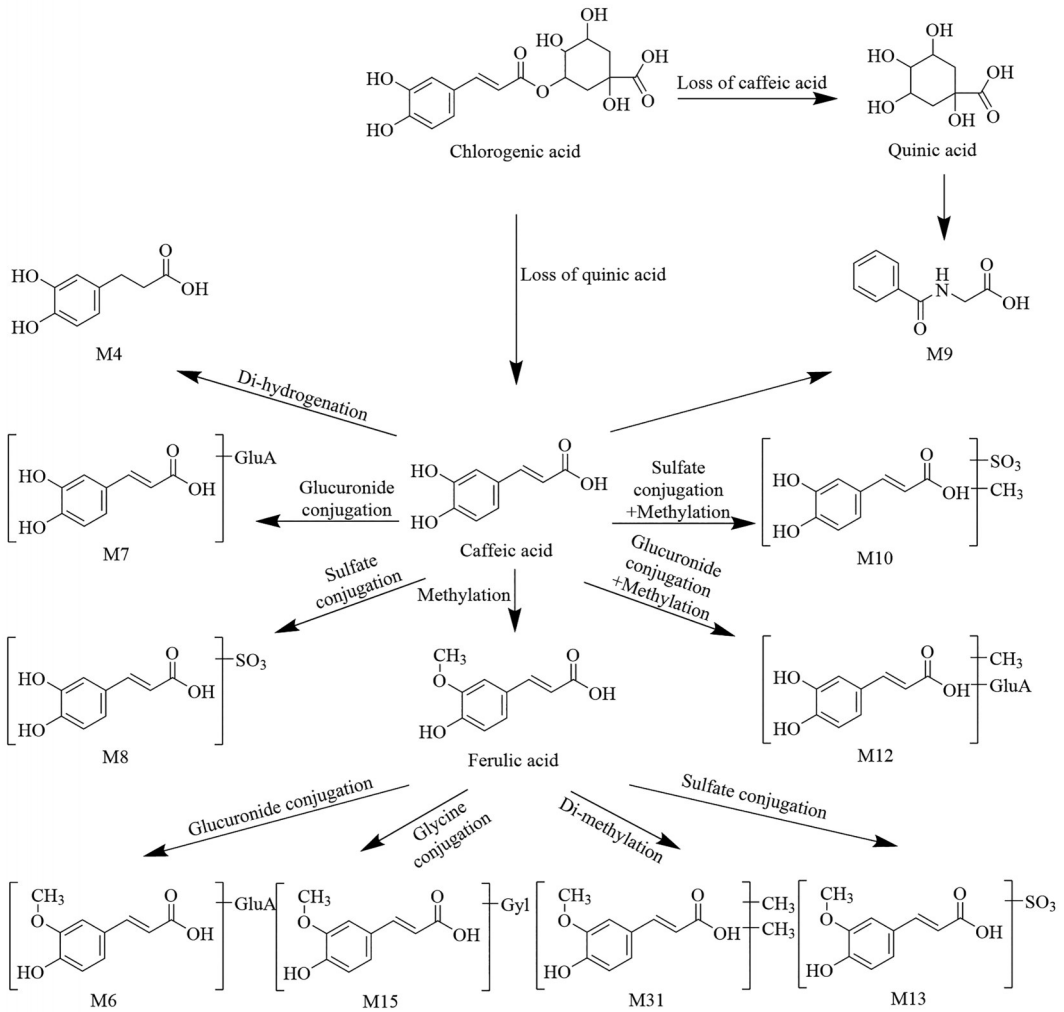


Figure 3 The possible metabolic pathways of organic acid-related metabolites in rats

4 网络药理学及分子对接

4.1 成分−靶点网络分析 结果显示, 数据库中筛选出296个化合物作用靶点, 构建“成分−靶点”网络(图4A)。

4.2 心肌梗死相关靶点的获取 获得XTS成分靶点与疾病共同靶点234个。

4.3 PPI网络分析 Cytoscape 3.9.1软件分析获得47个核心靶点。构建PPI网络(图4B), 提示EGFR、MMP9、PTGS2、IL1B、STAT3等, 可能是XTS治疗心肌梗死的关键靶点。

4.4 GO和KEGG通路富集分析 GO功能富集得到1 123个条目, 提示XTS治疗心肌梗死主要以磷酸化作用、炎症反应、对细胞凋亡过程的负向调节为主的生物过程(BP), 以细胞质、细胞表面为主的细胞组分(CC)和以相同蛋白结合、ATP结合为主的分子功能(MF)(图4C); KEGG信号通路分析结果表明XTS治疗心肌梗死可能与PI3K/AKT通路、脂质和动脉粥样硬化, 流体剪切力与动脉粥样硬化、MAPK信号通路、AGE-RAGE信号通路等密切相关(图4D)。

4.5 药物−成分−通路−靶点−疾病网络构建 通过DAVID数据库分析, 得到前20个核心通路, 构建“药物−成分−通路−靶点−疾病”网络(图4E)。提示阿魏酸、异阿魏酸、咖啡酸、绿原酸、香草酸、洋川芎内酯A、洋川芎内酯F、苯甲酰芍药苷等为心肌保护的主要活性成分。

4.6 分子对接结果及可视化验证 分子对接结果表明, 配体与受体之间均能生成氢键, 且部分对接结果存在配体与受体的多个氨基酸残基相连的现象(图5), 表明核心成分与核心靶点之间具有较高的生物活性。

讨论

临床上, XTS用于治疗心血瘀阻所致冠心病、心绞痛、心肌梗死等疾病。但XTS的成分复杂, 治疗心肌梗死的药效物质基础尚未明确, 不利于其临床应用和深入研究。因此, 本研究首次分析了入血成分及代谢

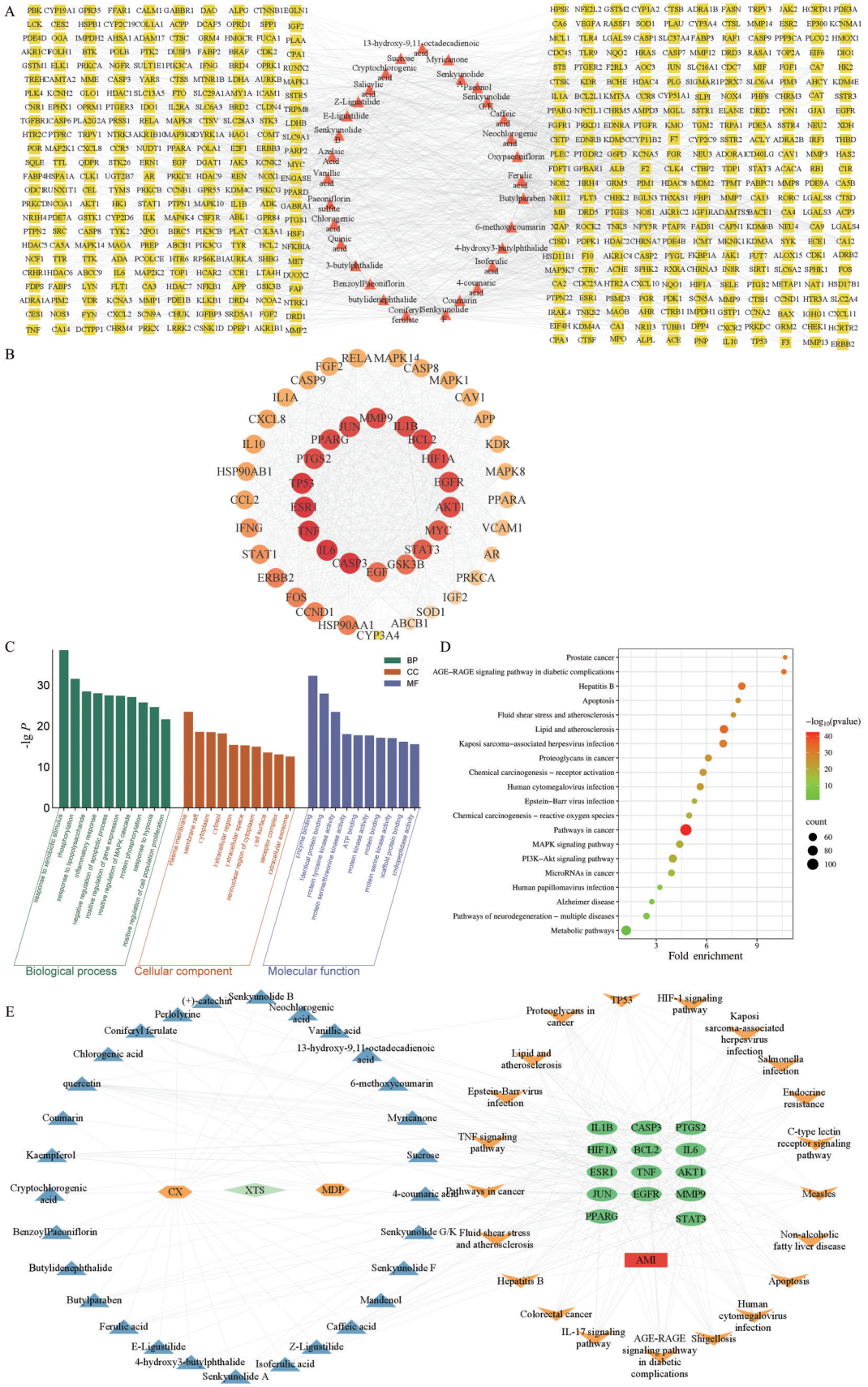


Figure 4 Results of network pharmacology analysis. A: Compound-target network; B: Protein-protein interaction network; C: GO analysis of AMI treated with cardiac pain relief spray; D: KEGG analysis of AMI treated with cardiac pain relief spray; E: Network of component-target-pathway-disease

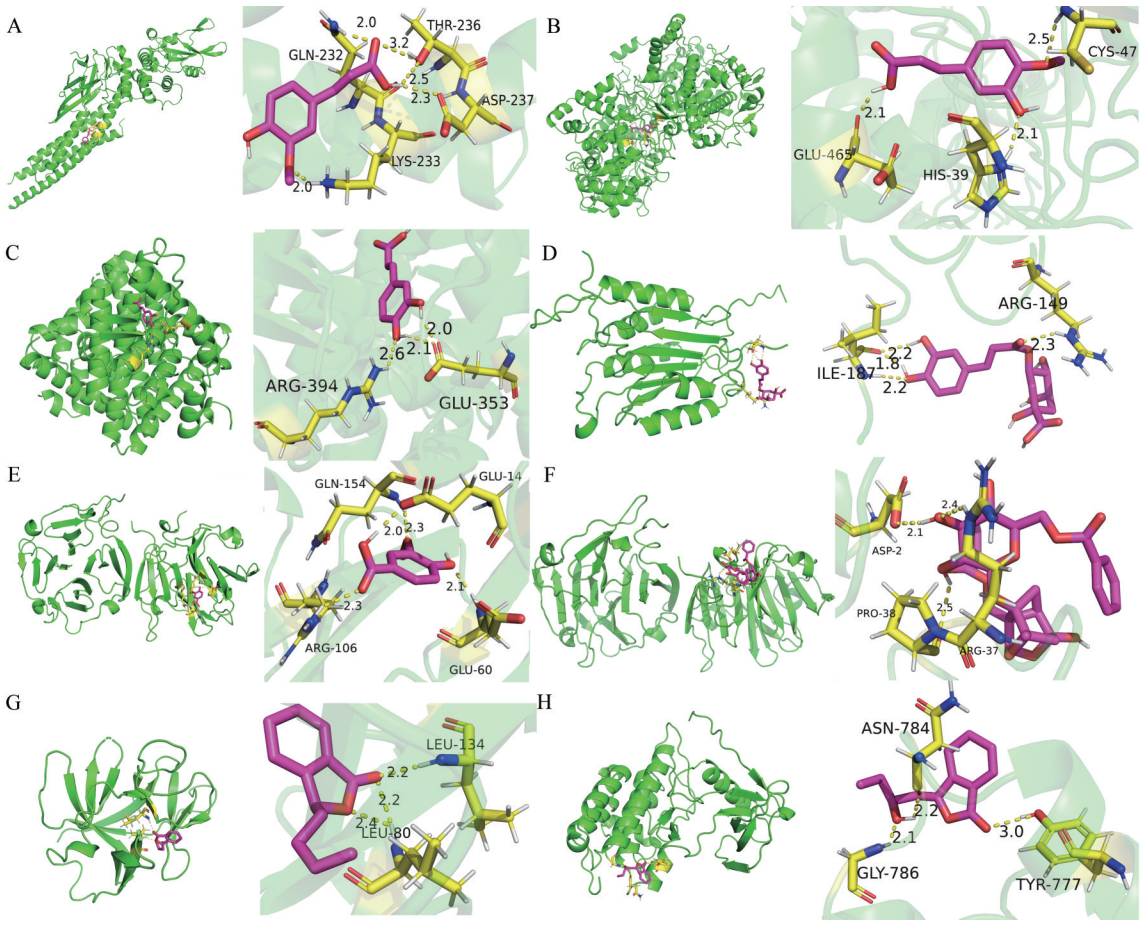


Figure 5 Molecular docking diagrams of key active ingredients binding to core targets. A: Ferulic acid and STAT3; B: Isoferulic acid and PTGS2; C: Caffeic acid and ESR1; D: Chlorogenic acid and CASP3; E: Vanillic acid and MMP9; F: Benzoylpaeoniflorin and MMP9; G: Senkyunolide A and IL1B; H: Senkyunolide F and EGFR

产物, 结合网络药理学及分子对接等探讨XTS治疗AMI的作用靶点, 为XTS的后续研究与临床应用提供数据支持。

本研究采用UPLC-Orbitrap-HRMS技术, 从XTS鉴定出41个入血原型成分, 并结合网络药理学对XTS的潜在活性成分进行分析预测, XTS治疗AMI的8个关键活性成分为阿魏酸、异阿魏酸、绿原酸、咖啡酸、香草酸、洋川芎内酯A、洋川芎内酯F、苯甲酰芍药苷。其中阿魏酸具有很强的抗氧化和细胞保护活性, 可减少梗死面积, 并改善心脏功能[28]; 绿原酸可以减轻ISO诱导的ERS和心脏肥大[29]; 咖啡酸通过抑制转化生长因子β-1受体信号通路来减轻心肌纤维化并改善心肌梗死后心脏功能[15]; 香草酸可抑制异丙肾上腺素诱导的心肌梗死大鼠的Fas受体和caspase介导的细胞凋亡信号通路和心肌细胞死亡[30]; 洋川芎内酯A对大鼠主动脉血管具有舒张作用[31]; 苯甲酰芍药苷可通过促进Nrf2/HO-1通路抑制AMI模型大鼠的心肌细胞凋亡, 并发挥保护心功能的作用[32]。

本研究的PPI分析结果显示EGFR、MMP9、PTGS2、IL1B、STAT3、ESR1、CASP3为活性成分相关联的核心靶点, 这些靶点大多与细胞凋亡、细胞分化、炎症反应等相关。在Grisanti等[33]研究中, EGFR已被证明可被GPCR反式激活作用影响心脏重塑, 以及心脏肥厚和纤维化; Becirovic等[34]研究中描述了MMP-9水平与心肌梗死死亡率和左心室重构和功能障碍之间的联系; Zhou等[35]研究发现, 动脉粥样硬化的严重程度与PTGS2水平有正相关联系; Mai等[36]研究证明了靶向IL-1β先天免疫途径的canakinumab抗炎疗法可以显著降低心血管事件复发的发生率, 表明IL-1β在动脉粥样硬化中起重要作用; Zhuang等[37]研究揭示了DYRK1B-STAT3通过损害线粒体生物能量学驱动心脏肥大和心力衰竭的作用机制; Chen等[38]研究通过黄芪调节ESR1的表达对心力衰竭的心脏产生了保护作用; Ruetten等[39]研究证实了抑制caspase-3可显著改善心肌梗死的缺血后收缩恢复。

分子对接的结果表明, XTS的关键活性成分与关

键靶点可自由结合 (结合能 ≤ −5.00 kcal·mol^{-1}), 进一步验证了网络药理学分析结果的可靠性。为XTS中活性成分作用于AMI特定靶点的治疗提供了理论依据。

关键靶点的富集分析显示, XTS对AMI的治疗作用可能与PI3K/AKT、MAPK、AGE-RAGE等通路密切相关。研究表明, PI3K/Akt信号通路可调控一系列分子调节细胞存活、凋亡、生长、心脏收缩甚至相关基因的转录, 参与调节心脏纤维化的发生、进展和病理形成[40]; 通过调节AGE-RAGE信号通路可诱导氧化应激和心肌和血管组织的炎症[41]; 而抑制MAPK信号通路可缓解高脂饮食 (HFD) 诱导的心肌炎症、纤维化和肥大[42]。

综上所述, XTS可能通过新绿原酸、绿原酸、咖啡酸、4-香豆酸、6-甲氧基香豆素、阿魏酸、异阿魏酸、洋川芎内酯A、洋川芎内酯F、苯甲酰芍药苷等活性成分, 作用于EGFR、MMP9、PTGS2、IL1B、STAT3、ESR1、CASP3等关键靶点, 调控PI3K/AKT、MAPK、AGE-RAGE等通路对心血管产生调节作用, 初步揭示了XTS治疗心肌梗死的潜在物质基础及作用机制, 表明其治疗心肌梗死具有多成分、多靶点、多途径的特点。UPLC-Orbitrap-HRMS技术和网络药理学相结合可为进一步阐明XTS的作用机制提供依据。

作者贡献: 陆小龙负责完成实验, 数据分析及文章撰写; 梁万徽、苏梦负责部分数据处理及文章校对; 李龙飞、李平平、左池靖、张静参与了部分实验; 彭灿、张云静、王茜负责课题整体设计及文章修改。

利益冲突: 所有作者均声明不存在利益冲突。

References

[1] Wang XJ, Zhang BL. Elucidation of compatibility principle and scientific value of Chinese medical formulae based on pharmacometabolomics [J]. China J Chin Mater Med (中国中药杂志), 2010, 35: 1346-1348.

[2] Zhou MN, Chen XY, Chen XH, et al. Construction of "2R network pharmacology" research method for effective components of traditional Chinese medicine based on "prediction of dominant components-screening of potential targets" [J]. China J Chin Mater Med (中国中药杂志), 2021, 46: 2363-2369.

[3] Wang XJ. Progress in Analysis of Chinese Materia Medica [J]. World Sci Technol Mod Tradit Chin Med (世界科学技术-中医药现代化), 2002, 4: 1-4.

[4] Li HG, Hu SP, Zhou Y, et al. Pharmacology progress on the main bioactive components of *Ligusticum chuanxiong* Hort [J]. China J Clin Pharm Ther (中国临床药理学与治疗学), 2018, 23: 1302-1308.

[5] Yu W, Ilyas I, Aktar N, et al. A review on therapeutical potential of paeonol in atherosclerosis [J]. Front Pharmacol, 2022, 13: 950337.

[6] Wang J, Yan ML, Zhang M, et al. Study on the mechanism of "guiding action" of borneol in Suxiaojiuxin pills [J]. Acta Pharm Sin (药学学报), 2022, 57: 700-706.

[7] Wang CH, Zhao LC. Clinical observation on the treatment of angina pectoris in coronary heart disease with Xintongshu spray [J]. Clin J Tradit Chin Med (中医药临床杂志), 2000, 12: 75-76.

[8] Shen SG. Clinical and experimental study of 717 cases of angina pectoris in coronary heart disease treated with Xintongshu spray [J]. J Emerg Tradit Chin Med (中国中医急症), 1999, 8: 200-204.

[9] Ma JZ, Su C, Yang J, et al. Research advances on changes of myocardial metabolic patterns under physiological and pathological conditions [J]. Chin J Cardiovasc Med (中国心血管杂志), 2022, 27: 383-388.

[10] Liang WH, Tao SY, Zuo CJ, et al. HPLC fingerprint, content determination and transferring patterns of index components of Xintongshu spray [J]. China Pharm (中国药房), 2023, 34: 2861-2867.

[11] Li S, Liu H, Zhang C, et al. Serum pharmacochemistry and pharmacokinetics of major components after oral administration of Luhong recipe in rats using ultra-performance liquid chromatography-tandem mass spectrometry [J]. Biomed Chromatogr, 2022, 36: e5497.

[12] Tan Y, Huang Z, Liu Y, et al. Integrated serum pharmacochemistry, 16S rRNA sequencing and metabolomics to reveal the material basis and mechanism of Yinzhihuang granule against non-alcoholic fatty liver disease [J]. J Ethnopharmacol, 2023, 310: 116418.

[13] Xiong H, Li N, Zhao L, et al. Integrated serum pharmacochemistry, metabolomics, and network pharmacology to reveal the material basis and mechanism of Danggui Shaoyao San in the treatment of primary dysmenorrhea [J]. Front pharmacol, 2022, 13: 942955.

[14] Lai YN, Zhan SF, Liu XH, et al. Exploring the effects and dispensing pattern of San Ye Tang for the treatment of cough based on network pharmacology [J]. Chin Tradit Patent Med (中成药), 2021, 43: 1072-1081.

[15] Jiang W, Deng B, Xie M, et al. Caffeic acid mitigates myocardial fibrosis and improves heart function in post-myocardial infarction by inhibiting transforming growth factor-β receptor 1 signaling pathways [J]. Biomed Pharmacother, 2024, 177: 117012.

[16] Wang Q, Chen G, Chen X, et al. Development of a three-step-based novel strategy integrating DMPK with network pharmacology and bioactivity evaluation for the discovery of Q-markers of traditional Chinese medicine prescriptions: Danlou tablet as an example [J]. Phytomedicine, 2023, 108: 154511.

[17] Li J, Wang SP, Wang YQ, et al. Comparative metabolism study on chlorogenic acid, cryptochlorogenic acid and neochlorogenic

acid using UHPLC-Q-TOF MS coupled with network pharmacology [J]. China J Chin Mater Med (中国中药杂志), 2021, 19: 212-224.

[18] Naranjo Pinta M, Montoliu I, Aura AM, et al. *In vitro* gut metabolism of [U-^{13}C]-quinic acid, the other hydrolysis product of chlorogenic acid [J]. Mol Nutr Food Res, 2018, 62: e1800396.

[19] Zhang JJ, Luo QS, Li QQ, et al. Study of plasma major metabolites and bioavailability of chlorogenic acid after oral administration to rats in two physiological states of fasted and non-fasted [J]. Acta Agric Univ Jiangxiensis (江西农业大学学报), 2022, 44: 1229-1238.

[20] Jin HT, Liu JT, Wang JF, et al. Identification of absorbed components in rat plasma after oral administration of Yuxingcao mixture by UPLC-Q-TOF/MS [J]. Chin Tradit Herb Drugs (中草药), 2021, 52: 2890-2896.

[21] Shi JC, Fei K, Zhang WZ, et al. Serum pharmacochemistry of Astragalus Vermiculatus hypoglycemic capsules based on UPLC-QE-Orbitrap-MS method [J]. Chin Tradit Pat Med (中成药), 2023, 45: 2414-2419.

[22] Zhang YY, Wu LP, Feng YF, et al. Identification of metabolites of Yiqi Baoyuan Prescription in rat plasma, bile, urine and feces after oral administration [J]. China J Chin Mater Med (中国中药杂志), 2022, 47: 4469-4479.

[23] Li F, Li J, Wang YQ, et al. Metabolite identification of cryptochlorogenic acid in rats using UHPLC-Q-TOF MS [J]. Chin Tradit Herb Drugs (中草药), 2021, 52: 3810-3817.

[24] Gao X, Li Y, Meng M, et al. Exploration of chemical composition and absorption characteristics of Chaigui granules based on UHPLC-Q-orbitrap-MS/MS[J]. J Pharm Biomed Anal, 2020, 187: 113293.

[25] Li J, Liu ZH, Dong F, et al. Metabolite identification of neochlorogenic acid in rats based on UPLC-Q-TOF MS [J]. Mod Chin Med (中国现代中药), 2020, 22: 1048-1055, 1071.

[26] Yang YT, Li ZL, Zhou L, et al. Metabolites identification and metabolic pathway analysis of Shenkang Injection in rats based on UHPLC-Q-Orbitrap HRMS [J]. Chin Tradit Herb Drugs (中草药), 2024, 55: 730-745.

[27] He Y, Su W, Chen T, et al. Identification of prototype compounds and derived metabolites of naoxintong capsule in Beagle dog urine and feces by UFLC-Q-TOF-MS/MS [J]. J Pharm Biomed Anal, 2019, 176: 112806.

[28] Li C, Chen L, Song M, et al. Ferulic acid protects cardiomyocytes from TNF-*α*/cycloheximide-induced apoptosis by regulating autophagy [J]. Arch Pharm Res, 2020, 43: 863-874.

[29] Ping P, Yang T, Ning C, et al. Chlorogenic acid attenuates cardiac hypertrophy *via* up-regulating sphingosine-1-phosphate receptor1 to inhibit endoplasmic reticulum stress [J]. ESC Heart Fail, 2024, 11: 1580-1593.

[30] Stanely Mainzen Prince P, Dhanasekar K, Rajakumar S. Vanillic acid prevents altered ion pumps, ions, inhibits Fas-receptor and caspase mediated apoptosis-signaling pathway and cardiomyocyte death in myocardial infarcted rats [J]. Chem Biol Interact, 2015, 232: 68-76.

[31] Chan SS, Cheng TY, Lin G. Relaxation effects of ligustilide and senkyunolide A, two main constituents of Ligusticum chuanxiong, in rat isolated aorta [J]. J Ethnopharmacol, 2007, 111: 677-680.

[32] Yu L, Wu Y. Effects of benzoylpaeoniflorin on cardiac function in rats with myocardial infarction *via* promoting Nrf2/HO-1 pathway [J]. Lab Anim Sci (实验动物科学), 2022, 39: 44-48.

[33] Grisanti LA, Guo S, Tilley DG. Cardiac GPCR-mediated EGFR transactivation: impact and therapeutic implications [J]. J Cardiovasc Pharmacol, 2017, 70: 3-9.

[34] Becirovic-Agic M, Chalise U, Daseke MJ, et al. Infarct in the heart: what's MMP-9 got to do with it? [J]. Biomolecules, 2021, 11: 491.

[35] Zhou Y, Zhou H, Hua L, et al. Verification of ferroptosis and pyroptosis and identification of PTGS2 as the hub gene in human coronary artery atherosclerosis [J]. Free Radical Biol Med, 2021, 171: 55-68.

[36] Mai W, Liao Y. Targeting IL-1beta in the treatment of atherosclerosis [J]. Front Immunol, 2020, 11: 589654.

[37] Zhuang L, Jia K, Chen C, et al. DYRK1B-STAT3 drives cardiac hypertrophy and heart failure by impairing mitochondrial bioenergetics [J]. Circulation, 2022, 145: 829-846.

[38] Chen Q, Wang J, Sun L, et al. Mechanism of *Astragalus membranaceus* (Huangqi, HQ) for treatment of heart failure based on network pharmacology and molecular docking [J]. J Cell Mol Med, 2024, 28: e18331.

[39] Ruetten H, Badorff C, Ihling C, et al. Inhibition of caspase-3 improves contractile recovery of stunned myocardium, independent of apoptosis-inhibitory effects [J]. J Am Coll Cardiol, 2001, 38: 2063-2070.

[40] Qin W, Cao L, Massey IY. Role of PI3K/Akt signaling pathway in cardiac fibrosis [J]. Mol Cell Biochem, 2021, 476: 4045-4059.

[41] Wasim R, Mahmood T, Siddiqui MH, et al. Aftermath of AGE-RAGE cascade in the pathophysiology of cardiovascular ailments [J]. Life Sci, 2022, 307: 120860.

[42] Chen Y, Lin W, Zhong L, et al. Bicyclol attenuates obesity-induced cardiomyopathy *via* inhibiting NF-*κ*B and MAPK signaling pathways [J]. Cardiovasc Drugs Ther, 2023, 37: 1131-1141.